

## Precipitation impacts on vegetation spring phenology on the Tibetan Plateau

**Running title:** Spring phenology on Tibetan Plateau

1

2 Miaogen Shen<sup>1,2\*</sup>, Shilong Piao<sup>1,2</sup>, Nan Cong<sup>1</sup>, Gengxin Zhang<sup>1</sup>, Ivan A Jassens<sup>3</sup>

3 1, Key Laboratory of Alpine Ecology and Biodiversity, Institute of Tibetan Plateau Research,

4 Chinese Academy of Sciences, 16 Lincui Road, Chaoyang District, Beijing, China

5 2, CAS Center for Excellence in Tibetan Plateau Earth Sciences, Beijing, China

6 3, Centre of Excellence PLECO (Plant and Vegetation Ecology), Department of Biology,

7 University of Antwerp, Wilrijk, Belgium

8

9 \*Author for correspondence, Institute of Tibetan Plateau Research, Chinese Academy of

10 Sciences, No. 16 Lincui Rd., Chaoyang District, Beijing, 100101, China, Email:

11 [shenmiaogen@itpcas.ac.cn](mailto:shenmiaogen@itpcas.ac.cn), Tel: +8610-84097043, Fax: +8610-84097079

**12 Abstract**

13 The ongoing changes in vegetation spring phenology in temperate/cold regions are widely  
14 attributed to temperature. However, in arid/semiarid ecosystems the correlation between  
15 spring temperature and phenology is much less clear. We test the hypothesis that precipitation  
16 plays an important role in the temperature dependency of phenology in arid/semi-arid regions.  
17 We therefore investigated the influence of pre-season precipitation on satellite-derived  
18 estimates of starting date of vegetation growing season (SOS) across the Tibetan Plateau (TP).  
19 We observed two clear patterns linking precipitation to SOS. First, SOS is more sensitive to  
20 inter-annual variations in pre-season precipitation in more arid than in wetter areas. Spatially,  
21 an increase in long-term averaged pre-season precipitation of 10 mm corresponds to a decrease  
22 of the precipitation sensitivity of SOS by about  $0.01 \text{ day mm}^{-1}$ . Second, SOS is more  
23 sensitive to variations in pre-season temperature in wetter than in dryer areas of the plateau. A  
24 spatial increase in precipitation of 10 mm corresponds to an increase in temperature  
25 sensitivity of SOS of  $0.25 \text{ day } ^\circ\text{C}^{-1}$  (0.25-day SOS advance per  $1\text{-}^\circ\text{C}$  temperature increase).  
26 Those two patterns indicate both direct and indirect impacts of precipitation on SOS on TP.  
27 This study suggest a balance between maximizing benefit from the limiting climatic resource  
28 and minimizing the risk imposed by other factors. In wetter areas, the lower risk of drought  
29 allows greater temperature sensitivity of SOS to maximize the thermal benefit, which is  
30 further supported by the weaker inter-annual partial correlation between growing degree days  
31 and pre-season precipitation. In more arid areas, maximizing the benefit of water requires  
32 greater sensitivity of SOS to precipitation, with reduced sensitivity to temperature. This study  
33 highlights the impacts of precipitation on SOS in a large cold and arid/semiarid region and

34 suggests that influences of water should be included in SOS module of terrestrial ecosystem

35 models for drylands.

36

37 **Key words:** climate change, precipitation, sensitivity, temperature, Tibetan Plateau,

38 vegetation spring phenology

## 39 **Introduction**

40 The starting date of the vegetation growing season (SOS) in temperate and boreal regions has  
41 received particular attention, because of its strong response to climate change and its strong  
42 impacts on ecosystem processes, such as energy exchange, hydrological cycle, and carbon  
43 uptake (Badeck *et al.*, 2004, Barr *et al.*, 2009, Cleland *et al.*, 2007, Obrist *et al.*, 2003, Piao *et*  
44 *al.*, 2007, Richardson *et al.*, 2010, Richardson *et al.*, 2013). Changes in SOS and their relation  
45 to the temperature rise during the past few decades have been well documented. For instance,  
46 Menzel *et al.* (2006) suggested that European phenology changes matched the ongoing  
47 warming pattern and Fu *et al.* (2014a) showed that the absence of further winter warming in  
48 recent years was reflected in homeostasis of spring phenology of early-spring species, while  
49 later-spring species continued to exhibit earlier leaf flushing in response to the continued  
50 warming trend in later spring.

51

52 Less attention has been devoted to the variability in the temperature dependency of SOS  
53 across a range of temperatures (Hwang *et al.*, 2014, Penuelas *et al.*, 2004). Recently, it was  
54 shown that the inter-annual relationships between temperature and SOS varied noticeably  
55 among different areas. For example, Jeong *et al.* (2011) found that the correlation coefficient  
56 between SOS and preseason mean temperature varied from  $-0.3$  to  $-0.7$  across the Northern  
57 Hemisphere, and that in central Eurasia faster warming did not necessarily induce greater  
58 SOS advance. Such a 'mismatch' was consistent with a recent study that indicated that the  
59 sensitivity of SOS to inter-annual variations in preseason mean temperature varied  
60 dramatically over the Northern Hemisphere (Shen *et al.*, 2014a). The temperature sensitivity

61 of vegetation spring phenology, defined as the change in SOS per unit change in  
62 spring-temperature, is one of the most important keys to understanding the relationship  
63 between vegetation phenology and temperature change, and to project phenological changes  
64 in response to future climate change. However, the sensitivity of phenology to temperature  
65 change, and especially the regional differences in temperature sensitivity, is not yet fully  
66 understood.

67

68 While temperature plays an important role, other environmental factors may also affect SOS.  
69 Water is needed for sustaining plant growth, indicating that variability in SOS might be  
70 potentially related to optimal water conditions, particularly in the arid/semiarid areas. For  
71 example, Zhang *et al.* (2005) showed that the spatial variation in SOS closely tracked the  
72 onset of the rainy season in Africa, where temperature is a less limiting factor. In dry  
73 temperate/cold regions with wet winters, SOS may not be closely related to water conditions,  
74 because these tend to be optimal after winter. In contrast, in dry temperate/cold areas with dry  
75 winters and wetter summers, pre-season precipitation determines water availability in spring  
76 and may therefore affect SOS (Chen *et al.*, 2014). Hence, Cong *et al.* (2013) argued that the  
77 sensitivity of SOS to temperature was likely to be smaller in areas with less pre-season  
78 precipitation in temperate China. In the temperate grasslands of Northeast China, green-up  
79 onset was indeed advanced during years with higher soil moisture (Liu *et al.*, 2013). However,  
80 in a semiarid phenological garden (with an annual precipitation of 570 mm) in central China  
81 with dry winters, leaf flushing was later after wetter winters than after drier winters in 34 out  
82 of 42 species (23 being significant at  $P < 0.05$  level) and no single significantly negative

83 correlation was observed between the first leafing date and the preseason precipitation (Dai *et*  
84 *al.*, 2013). Moreover, it was reported that larger amounts of preseason precipitation may  
85 increase the heat demand (growing degree days) for SOS (Fu *et al.*, 2014b), indicating that  
86 precipitation could exert other, indirect, impacts on spring phenology. The studies above  
87 suggest that preseason precipitation clearly can influence SOS, but also that there can be  
88 diverse responses of SOS to preseason precipitation even in arid/semiarid regions, rendering  
89 the sensitivity of SOS to preseason temperature even more complex.

90

91 Most areas of the Tibetan Plateau (TP) are characterized by an arid/semiarid climate, with  
92 annual precipitation ranging from dozens to hundreds of millimeters, and rainfall occurring  
93 mainly in the growing season from May to September (Gao & Liu, 2013). Controversy still  
94 exists about the effects of precipitation on spring phenology on the TP. For example, Piao *et al.*  
95 (2006) suggested that increased preseason precipitation likely postponed SOS for alpine  
96 meadows and tundra in the TP, whereas Shen *et al.* (2014b) attributed delayed SOS to  
97 declines in preseason precipitation. The TP differs from the above reviewed dry temperate  
98 regions mainly because it is colder, with mean annual temperature ranging between  $-15\text{ }^{\circ}\text{C}$   
99 and  $10\text{ }^{\circ}\text{C}$  (You *et al.*, 2013). Variation in vegetation growth and in spring phenology is  
100 therefore strongly controlled by temperature (Kato *et al.*, 2006, Piao *et al.*, 2011, Tan *et al.*,  
101 2010, Wang *et al.*, 2012). In this study, we aim to elucidate the effects of precipitation on  
102 inter-annual changes in SOS across the TP and on the response of SOS to temperature, and  
103 discuss the potential underlying mechanisms.

104

105 **Materials and methods**

106 *Retrieving SOS using greenness vegetation index*

107 Greenness vegetation indices, including NDVI and enhanced vegetation index (EVI), have  
108 been shown sensitive indicators of canopy parameters, such as leaf area index and  
109 aboveground green biomass (Di Bella *et al.*, 2004, Shen *et al.*, 2008, Shen *et al.*, 2010, Tucker  
110 *et al.*, 1986, Wylie *et al.*, 2002), and are therefore widely used to derive vegetation phenology  
111 (Ganguly *et al.*, 2010, Garonna *et al.*, 2014, Myneni *et al.*, 1997, Shen *et al.*, 2012, Zhang *et*  
112 *al.*, 2013). We used NDVI derived from the observations by the sensor VEGETATION  
113 onboard Système Pour l'Observation de la Terre (SPOT NDVI) and MODerate resolution  
114 Imaging Spectroradiometer (MODIS NDVI and MODIS EVI) to determine SOS from 2000 to  
115 2012 in the TP. We did not include the NDVI from Advanced Very High Resolution  
116 Radiometer (AVHRR), because it has been reported to have low quality on the western TP for  
117 this period (Zhang *et al.*, 2013). The SPOT NDVI was produced at a spatial resolution of 1  
118 km using the 10-day maximum-value composition technique (i.e., by selecting the highest  
119 NDVI value from each period of 10 days), and the MODIS NDVI and EVI were produced at  
120 500-m resolution and 16-day compositing period. The effects of satellite orbit shift and sensor  
121 degradation have been removed and the atmospheric contaminations of water vapor, ozone  
122 and aerosols have also been eliminated, both following standard procedures (Huete *et al.*,  
123 2002, Maisongrande *et al.*, 2004, Rahman & Dedieu, 1994). Effects of snow cover on NDVI  
124 and EVI for each pixel were further eliminated by using the median value of the  
125 uncontaminated winter NDVI (EVI) values (MOD13A1-Quality, 2011, VGT-FAQ, 2012)  
126 between November and the following March (Ganguly *et al.*, 2010, Zhang *et al.*, 2006, Zhang

127 *et al.*, 2007). After that, abrupt drops of NDVI (EVI) value before the occurrence of the  
128 annual NDVI (EVI) maximum in summer were replaced by the value reconstructed using the  
129 Savitzky–Golay filter (Chen *et al.*, 2004), because clouds and poor atmospheric conditions  
130 usually depress NDVI (EVI) values.

131

132 Next, four methods were used to determine SOS from the time series of each of the three  
133 vegetation indices, including two inflection point-based methods ( $CCR_{\max}$  and  $\beta_{\max}$ ) and two  
134 threshold-based methods ( $G_{20}$  and  $CR_{\max}$ ). Taking NDVI as example, in the  $CCR_{\max}$  method,  
135 SOS was determined as the date when the rate of change of curvature of the logistic function  
136 curve fitted to NDVI reaches its first local maximum value (Zhang *et al.*, 2003). In the  $\beta_{\max}$   
137 method, SOS was calculated as the date when NDVI increases at the highest rate in a year  
138 (Studer *et al.*, 2007). In the  $G_{20}$  method, SOS was the first day in the ascending period when  
139 NDVI increased above 20% of its annual range (Yu *et al.*, 2010). When applying the  $RC_{\max}$   
140 method, SOS was the date when NDVI first reaches a predefined absolute threshold that  
141 corresponds to the maximum rate of changes in the average seasonal NDVI curve in spring  
142 (Piao *et al.*, 2006). Detailed descriptions of those four methods are given in Shen *et al.*  
143 (2014b). We calculated the temporal trend of SOS determined for each method and vegetation  
144 index using linear regression between SOS and year order, and found a broadly consistent  
145 spatial pattern of trends across all the vegetation indices and methods [similar to Fig. 4 in  
146 Shen *et al.* (2014b)]. We hence used averaged SOS over all the three vegetation indices and  
147 four methods in the following analyses.

148



149 *Analyses*

150 Considering that both preseason precipitation and temperature may affect SOS, its sensitivity  
151 to preseason mean temperature (Ta) and to cumulative precipitation (PPT) was defined  
152 respectively as the coefficients of Ta and PPT using the multiple linear regression in which  
153 SOS was set the dependent variable and Ta and PPT the independent variables for each pixel.  
154 Since the length of the preseason period for Ta or PPT could vary among different areas  
155 (Jeong *et al.*, 2011, Shen *et al.*, 2011), we did not use a fixed period. Instead, we used an  
156 optimization method to determine the preseason period length for Ta and PPT for each pixel  
157 using a linear regression. In the optimization process, we minimized the root mean of squared  
158 errors (RMSE) between observed and predicted SOS by using Ta and PPT for periods of  
159 different lengths preceding the 2000-2012 average of SOS. Here, a step of 10 days was used  
160 when changing the preseason period length to smooth potential extreme values. We did not  
161 constrain that the preseason length for Ta is identical to that for PPT. After having determined  
162 the optimal preseason length for each pixel, preseason temperature and precipitation, and the  
163 sensitivity of SOS to these climatic variables were determined. For each pixel, we used the  
164 preseason precipitation averaged for 2000-2012 to present its preseason water availability, i.e.,  
165 areas with more long-term average precipitation were considered wetter.

166

167 We next investigated whether or not precipitation would indirectly affect SOS by altering the  
168 heat requirement of plant seasonal development. The heat requirement is expressed in  
169 growing degree days (GDD), which is a widely used method to assess the effect of  
170 temperature on plant development (e.g. Botta *et al.*, 2000, Chuine, 2000, Fu *et al.*, 2014b,

171 Hanninen & Kramer, 2007, Jeong *et al.*, 2012, Zhang *et al.*, 2007). We analyzed the effect  
172 of precipitation on GDD using the inter-annual partial correlation between the preseason  
173 precipitation and GDD and setting the number of chilling days (CD) as the control variable.  
174 The latter was done to remove the potential effects of CD on GDD, because previous studies  
175 showed a negative correlation between GDD and CD (Murray *et al.*, 1989, Zhang *et al.*, 2004).  
176 This partial correlation method has been successfully applied to remove the covariate effects  
177 between multiple influential factors in ecological studies (Beer *et al.*, 2010, Fu *et al.*, 2014b,  
178 Peng *et al.*, 2013). Here, GDD was the sum of daily mean temperature exceeding 0 °C from  
179 January 1<sup>st</sup> to the day before SOS. CD was the number of days with daily mean temperature  
180 below 0 °C from September 1<sup>st</sup> in the previous year to SOS.

181

182 To examine whether or not SOS is more sensitive to preseason temperature in wetter than in  
183 dryer areas, spatial partial correlation analysis was conducted between the temperature  
184 sensitivity of SOS and the long-term average precipitation data, while setting mean annual  
185 temperature (MAT) over 2000-2012 and mean CD over 2000-2012 as the control variables. In  
186 parallel, spatial partial correlation analysis was performed between precipitation sensitivity of  
187 SOS and the long-term average precipitation, again while accounting for MAT and CD. We  
188 also investigated the spatial variability in the precipitation effect on the heat requirement in  
189 relation to water condition. This was achieved using spatial partial correlation between the  
190 inter-annual partial correlation coefficient between the preseason precipitation and GDD and  
191 the long-term average precipitation, with MAT and CD being the control variables. Last, we  
192 applied spatial partial correlation analysis between GDD and the long-term average

193 precipitation accounting for MAT and CD, to examine whether or not GDD requirement is  
194 higher in wetter areas.

195

196 The above analyses were conducted twice, first on all pixels across the plateau and second on  
197 only those pixels that were equipped with a meteorological station, which occurred  
198 predominantly in the eastern and central parts of the TP (Fig. 1b). For these latter station-level  
199 analyses, we used daily temperature and precipitation records from 1999 to 2012 for 80  
200 meteorological stations across the TP, which were provided by the China Meteorological  
201 Administration (CMA, <http://cdc.cma.gov.cn/index.jsp>). For the TP-wide analyses on all  
202 pixels, daily temperature and precipitation were calculated from a dataset developed by the  
203 Data Assimilation and Modeling Center for Tibetan Multi-spheres, Institute of Tibetan Plateau  
204 Research, Chinese Academy of Sciences (Chen *et al.*, 2011, He, 2010). The data were  
205 produced at a temporal resolution of 3 hours and spatial resolution of  $0.1^\circ \times 0.1^\circ$ , covering the  
206 entire mainland of China. Air temperature at 1.5 m was produced by merging the observations  
207 collected at 740 operational stations of CMA into the corresponding Princeton meteorological  
208 forcing data (Sheffield *et al.*, 2006). Precipitation was produced by combining three datasets,  
209 including the Tropical Rainfall Measuring Mission (TRMM) 3B42 precipitation products  
210 (Huffman *et al.*, 2007), precipitation observations from 740 operational stations of CMA, and  
211 the Asian Precipitation – Highly Resolution Observational Data Integration Toward  
212 Evaluation of the Water Resources (APHRODITE) precipitation data (Yatagai *et al.*, 2009).

213

214 **Results**

215 *Spatial distribution of sensitivity of SOS to pre-season temperature and precipitation*

216 The temperature sensitivity of SOS, determined by a multiple regression, was negative in  
217 approximately 77% of the TP area, especially in the central, eastern, and northeastern parts  
218 (Fig. 1a). This temperature sensitivity was significantly negative ( $P < 0.05$ , T-test) in about  
219 37% of the pixels. The temperature sensitivity exceeded (was lower than)  $-4 \text{ day } ^\circ\text{C}^{-1}$ , i.e. an  
220 increase in pre-season temperature of  $1 \text{ } ^\circ\text{C}$  corresponded to a SOS advance of at least 4 days,  
221 in nearly 39% of the area. In contrast to this majority of pixels exhibiting the expected  
222 advance of SOS with warming, much less positive temperature sensitivities were observed  
223 (Fig. 1a, right bottom inset). These occurred mainly in the southwestern plateau and in a few  
224 areas in the west and southwest of the Qinghai Lake and southeastern plateau. These positive  
225 temperature sensitivities ranged from 0 to  $+6 \text{ day } ^\circ\text{C}^{-1}$  (95% percentile) and were  
226 significantly positive ( $P < 0.05$ ) for only about 5% of the pixels. A briefly similar spatial  
227 pattern was also found for the temperature sensitivities of SOS calculated using the weather  
228 station data (Fig. 1b).

229

230 The precipitation sensitivity of SOS showed a strikingly different spatial pattern. In the  
231 southwestern plateau, the majority of pixels exhibited negative sensitivity values, mostly  
232 lower than  $-0.1 \text{ day mm}^{-1}$ , i.e. an increase in pre-season precipitation of 10 mm corresponded  
233 to a SOS advance of at least 1 day (Fig. 2a). Increases in pre-season precipitation were also  
234 likely to advance SOS in northeastern parts and a few of the central parts of the TP. In total,  
235 about 69% of the pixels showed negative precipitation sensitivity values, 23% being  
236 significant ( $P < 0.05$ ). On the other hand, positive precipitation sensitivity values were found

237 in about 31% of the TP; 5% being statistically significant ( $P < 0.05$ ), occurring mostly in the  
238 central plateau. The precipitation sensitivity calculated using weather station data also showed  
239 a roughly similar spatial pattern (Fig. 2b).

240

241 *Spatial variations in temperature and precipitation sensitivity of SOS in relation to climatic*  
242 *precipitation gradient*

243 We observed that, in general, SOS was more sensitive to inter-annual changes in pre-season  
244 mean temperature in the wetter areas (i.e., with higher long-term average precipitation) (Fig.  
245 3a). Spatially, an increase in long-term average precipitation of 10 mm corresponded to an  
246 increase in temperature sensitivity of  $0.25 \text{ day } ^\circ\text{C}^{-1}$ . The spatial variations in temperature  
247 sensitivity with regard to long-term average precipitation showed a similar pattern when we  
248 only included the pixels with a temperature sensitivity significant at  $P < 0.05$  level (grey line  
249 in Fig. 3a). Moreover, a significantly negative ( $P < 0.01$ ) spatial correlation between  
250 temperature sensitivity and long-term average precipitation was also found in a partial  
251 correlation analysis of the weather station observations in which MAT and CD were corrected  
252 for (Fig. 3a, left inset).

253

254 On the other hand, the precipitation sensitivity of SOS generally decreased from  $-0.14 \text{ day}$   
255  $\text{mm}^{-1}$  in the most arid area (receiving only 25 mm precipitation) to  $0 \text{ day mm}^{-1}$  in the areas  
256 with a long-term average precipitation of 150 mm or more (Fig. 3b). On average, an increase  
257 in long-term average precipitation of 10 mm corresponded to an increase in precipitation  
258 sensitivity of  $0.01 \text{ day mm}^{-1}$  within the areas with the precipitation ranging from 25 mm to

259 150 mm. The precipitation sensitivity variations also showed a similar decreasing pattern with  
260 regard to multi-yearly averaged precipitation when we only considered precipitation  
261 sensitivity significant at  $P < 0.05$  level (grey line in Fig. 3b). Further, the partial correlation  
262 analysis on the pixels with meteorological stations confirmed that the precipitation sensitivity  
263 of SOS weakens with increasing pre-season precipitation ( $P < 0.01$ ; Fig. 3b, inset).

264

#### 265 *Relationship between GDD and precipitation*

266 Because of the clear relationship between pre-season precipitation and the temperature  
267 sensitivity of SOS, we further investigated the inter-annual relationship between GDD and  
268 precipitation by performing a partial correlation analysis. As shown in Fig. 4a, the partial  
269 correlation was negative for 76% of the pixels across the TP, except for a few areas in the east  
270 of the plateau center. In particular in the southwestern plateau, the majority of the correlations  
271 was lower than  $-0.6$  ( $P < 0.05$ ). Significantly negative correlations were also found in many  
272 areas in the southeastern and northeastern plateau. Only about 2% of the pixels exhibited  
273 significantly positive ( $P < 0.05$ ) correlations. A similar spatial pattern of the partial  
274 correlations was found when analyzing the weather station data (Fig. 4b).

275

276 The partial correlation between pre-season precipitation and GDD was generally stronger  
277 (more negative) for areas with less precipitation, increasing from  $-0.4$  (on average) in areas  
278 with long-term average precipitation of about 25 mm to around  $-0.15$  in areas with a  
279 long-term precipitation of about 150 mm (Fig. 4c). Above this precipitation threshold, the  
280 correlation coefficient was very low, between  $-0.1$  to 0 (Fig. 4c). Indeed, statistically

281 significant (at  $P < 0.05$ ) partial correlation coefficients between GDD and precipitation were  
282 almost not observed in areas with more than 150 mm precipitation. Also across the weather  
283 stations, the partial correlation coefficient between GDD and precipitation tended to be  
284 stronger for areas with less precipitation ( $P < 0.05$ ; Fig. 4c, inset).

285

286 We also explored whether or not there was a spatial correlation between GDD and long-term  
287 averaged precipitation. To do this, we first calculated the average GDD over 2000-2012 for  
288 each pixel. As shown in Fig. 5a, average GDD was higher in the southwestern, southeastern,  
289 and northeastern parts of plateau, ranging from 200 to 500 °C-days (95% percentile) and was  
290 lower in the plateau center, mostly lower than 200 °C-days. Spatially, the GDD was lower in  
291 areas with less precipitation, decreasing from about 340 °C-days at a long-term average  
292 precipitation of 25 mm to about 150 °C-days at 150 mm (Fig. 5b), which is consistent with  
293 the negative inter-annual correlation between GDD and precipitation reported above. The  
294 weather stations-based analysis also revealed that the average GDD was spatially negatively  
295 related to long-term average precipitation ( $R = -0.55$ ,  $P < 0.01$ ) in the partial correlation  
296 between them by setting MAT and CD as controlling variables.

297

### 298 *Precipitation impact on SOS of different vegetation types*

299 On average, the alpine vegetation (including alpine tundra, alpine cushion, and alpine sparse  
300 vegetation; Editorial Board of Vegetation Map of China CAS (2001)) received the highest  
301 long-term average precipitation (90 mm), and had the highest temperature sensitivity of SOS  
302 ( $-3.3 \text{ day } ^\circ\text{C}^{-1}$ ), the lowest precipitation sensitivity of SOS ( $-0.024 \text{ day mm}^{-1}$ ), the weakest

303 inter-annual partial correlation between GDD and preseason precipitation ( $-0.18$ ), and the  
304 lowest GDD ( $155$  °C-days) among the three vegetation types (Fig. 6). In contrast, the steppe  
305 vegetation showed the exact opposite pattern, with the lowest long-term average precipitation  
306 ( $72$  mm), the lowest temperature sensitivity of SOS ( $-1.9$  day °C $^{-1}$ ), the greatest precipitation  
307 sensitivity of SOS ( $-0.108$  day mm $^{-1}$ ), the strongest inter-annual partial correlation between  
308 GDD and preseason precipitation ( $-0.44$ ), and the highest GDD ( $213$  °C-days). The third  
309 vegetation type, the meadows, received intermediate long-term average precipitation and  
310 exhibited intermediate values for the SOS-related variables too. Moreover, we found a similar  
311 pattern of the impacts of precipitation on SOS and its responses to the preseason climatic  
312 factors among the three vegetation types, when only focusing on the pixels with significant ( $P$   
313  $< 0.05$ ) sensitivities or partial correlations. Here we assume that the vegetation types do not  
314 change very much during the period of 2000-2012.

315

## 316 **Discussion**

317 Previous studies on phenology responses to climate warming in the TP have consistently  
318 shown SOS advances of about 2 weeks in the 1980s and 1990s (Piao *et al.*, 2011, Yu *et al.*,  
319 2010, Zhang *et al.*, 2013). Increasing spring temperature has been recognized as the major  
320 determinant of these SOS advances on the TP (Piao *et al.*, 2011, Shen *et al.*, 2014b). However,  
321 the potential impact of preseason precipitation was ignored in these previous studies. During  
322 2000-2011, despite continued spring warming, there has been no further regionally consistent  
323 advancing trend of SOS, with contrasting SOS patterns among the different areas of plateau  
324 (Shen *et al.*, 2014b). In this study, we used multivariate linear regression to incorporate the



325 effects of both preseason temperature and precipitation on SOS. The results indicated that, for  
326 a considerable area in southwestern TP, spring warming coincided with delayed SOS (Fig. 1).  
327 Moreover, across most of the TP, especially in the southwestern and northeastern plateau,  
328 increased preseason precipitation coincided with advanced SOS (Fig. 2). SOS on the TP is  
329 thus affected by both preseason temperature and precipitation, yielding spatially diverse SOS  
330 responses to climate change. Hence, analyses conducted at a regionally-aggregated level can  
331 not elucidate the real impacts of climate change on the SOS in the TP. Our results of the  
332 spatial pattern of SOS response to preseason temperature and precipitation may be taken to  
333 suggest that the regional-scale SOS advance in the 1980s and 1990s was likely the result of  
334 the combination of increasing temperature (Piao *et al.*, 2006) and fairly stable precipitation  
335 (Piao *et al.*, 2012, Xu *et al.*, 2008). In contrast, during 2000-2011 the decline in precipitation  
336 and further increase in temperature (Shen *et al.*, 2014b) did not significantly alter  
337 regional-level SOS during this period.

338

339 We observed that SOS sensitivity to both preseason temperature and precipitation varies  
340 greatly across the TP, with preseason precipitation affecting both these sensitivities. Water  
341 availability is thus an important determinant of the spatial pattern of SOS responses to climate  
342 change. In wetter areas, vegetation growth initiation is not limited by lack of water, and thus  
343 SOS can respond to temperature with greater sensitivity than to precipitation. In such areas,  
344 larger amounts of preseason precipitation would not advance SOS, but the accompanying  
345 deficient sunshine intensity and duration may retard SOS, either directly or indirectly by  
346 causing lower temperatures. In contrast, in more arid areas, soil moisture may still be

347 sub-optimal after winters with low rainfall, possibly explaining why SOS was less sensitive to  
348 temperature and more to preseason precipitation. Moreover, high preseason temperatures in  
349 these arid areas could even reduce water availability by increasing evapotranspiration and  
350 may thus even delay SOS (Yu *et al.*, 2003), explaining the unexpected positive temperature  
351 sensitivities of SOS that we observed for these dry regions in our analysis.

352

353 The current pattern of SOS sensitivity suggests that the TP vegetation tends to maximize the  
354 climatic benefit by making best use of climatic factors and meanwhile minimize the climatic  
355 risks. In wetter areas, where the risk of drought is lower, vegetation may have developed a  
356 greater temperature sensitivity of SOS to maximize the thermal benefit, a hypothesis that is  
357 further supported by the weaker inter-annual partial correlation between GDD and  
358 precipitation in those areas. In more arid areas, maximizing the usage of water (preseason  
359 precipitation) results in greater sensitivity of SOS to precipitation. We speculate that plants  
360 initiate their growth earlier if soil moisture becomes optimal earlier (more rainfall), even if  
361 temperatures are less optimal; in contrast, plants postpone SOS when soil moisture is still  
362 sub-optimal (low rainfall), even if GDD requirements have already been met.

363

364 To facilitate the greater precipitation sensitivity of SOS in dryer areas, heat should not be a  
365 limiting resource. For the mechanisms in the previous paragraph to function, vegetation in  
366 more arid areas should exhibit higher GDD requirements and a stronger negative inter-annual  
367 partial correlation between GDD and precipitation (i.e. greater GDD in years with less  
368 precipitation). The higher GDD requirement has the additional advantage of reducing the frost

369 risk. Hence, we hypothesize that there is a balance between maximizing the benefit from the  
370 limiting climatic resource and minimizing the risk imposed by other factors.

371

372 This study is the first to quantify the impacts of precipitation on SOS in one of the world's  
373 largest cold regions. Our results suggest that the projected warmer and slightly wetter future  
374 climate (IPCC, 2007) may generally favor earlier SOS on the TP. Meanwhile, attention should  
375 be paid to drought that could delay SOS and thus cause net carbon loss in warmer springs as  
376 ecosystem respiration can be elevated by higher temperature (Tan *et al.*, 2010). On the other  
377 hand, SOS delay of the grasslands could lead to foliage deficiency for yak and sheep and thus  
378 the local nomad's well-being (Klein *et al.*, 2014), highlighting the need of forecasting  
379 grassland SOS which could be improved by incorporating effects of precipitation.

380

381 Drylands cover about 41% of Earth's land surface (Reynolds *et al.*, 2007). For the  
382 arid/semiarid regions with dry and cold winter, such as the TP and north China (but probably  
383 also many other regions on Earth), both pre-season temperature and precipitation affect SOS,  
384 leading to a complex response of SOS to climate change. For these regions, the impacts of  
385 precipitation on SOS and on the SOS sensitivity to temperature should also be accounted for  
386 while assessing the vegetation phenological responses to climate change. If the conclusions  
387 obtained from this study are transferable to other winter-dry regions of the Earth, climatic  
388 warming may lead to greater SOS advance in relatively wetter areas than in dryer areas.  
389 Alternatively, in dry areas, especially where precipitation is not projected to increase, climatic  
390 warming may have smaller impact on SOS and might even delay SOS in the long term since

391 evapotranspiration may increase and permafrost may degrade (two processes that can  
392 decrease water availability). In addition, intra-seasonal changes in the timing and frequency of  
393 precipitation could also lead to SOS shifts. The impacts of precipitation on SOS are currently  
394 not included in the GDD- and/or CD-based phenology modules embedded in the  
395 state-of-the-art terrestrial biosphere models (Richardson *et al.*, 2012) that are used by the  
396 Intergovernmental Panel on Climate Change (IPCC), which may be a source of uncertainty in  
397 phenology model projections for drylands.

398

### 399 **Acknowledgements**

400 This work is funded by a “Strategic Priority Research Program (B)” of the Chinese Academy  
401 of Sciences (Grant No. XDB03030404), a National Basic Research Program of China (Grant  
402 No. 2013CB956303), and a grant from the National Natural Science Foundation of China (No.  
403 41201459). I.A.J. acknowledges support from the European Research Council Synergy grant  
404 610028.

405

### 406 **References**

- 407 Badeck FW, Bondeau A, Bottcher K, Doktor D, Lucht W, Schaber J, Sitch S (2004) Responses of spring phenology  
408 to climate change. *New Phytologist*, **162**, 295-309.
- 409 Barr A, Black A, McCaughey H (2009) *Climatic and phenological controls of the carbon and energy balances of*  
410 *three contrasting boreal forest ecosystems in Western Canada*, Heidelberg, Springer.
- 411 Beer C, Reichstein M, Tomelleri E *et al.* (2010) Terrestrial Gross Carbon Dioxide Uptake: Global Distribution and  
412 Covariation with Climate. *Science*, science.1184984.

- 413 Botta A, Viovy N, Ciais P, Friedlingstein P, Monfray P (2000) A global prognostic scheme of leaf onset using  
414 satellite data. *Global Change Biology*, **6**, 709-725.
- 415 Chen J, Jonsson P, Tamura M, Gu ZH, Matsushita B, Eklundh L (2004) A simple method for reconstructing a  
416 high-quality NDVI time-series data set based on the Savitzky-Golay filter. *Remote Sensing Of  
417 Environment*, **91**, 332-344.
- 418 Chen XQ, Li J, Xu L, Liu L, Ding D (2014) Modeling greenup date of dominant grass species in the Inner  
419 Mongolian Grassland using air temperature and precipitation data. *International Journal of  
420 Biometeorology*, **58**, 463-471.
- 421 Chen Y, Yang K, He J, Qin J, Shi J, Du J, He Q (2011) Improving land surface temperature modeling for dry land of  
422 China. *Journal of Geophysical Research*, **116**.
- 423 Chuine I (2000) A unified model for budburst of trees. *Journal of Theoretical Biology*, **207**, 337-347.
- 424 Cleland EE, Chuine I, Menzel A, Mooney HA, Schwartz MD (2007) Shifting plant phenology in response to global  
425 change. *Trends in Ecology & Evolution*, **22**, 357-365.
- 426 Cong N, Wang T, Nan H, Ma Y, Wang X, Myneni RB, Piao S (2013) Changes in satellite-derived spring vegetation  
427 green-up date and its linkage to climate in China from 1982 to 2010: a multi-method analysis. *Global  
428 Change Biology*, **19**, 881-891.
- 429 Dai JH, Wang HJ, Ge QS (2013) Multiple phenological responses to climate change among 42 plant species in  
430 Xi'an, China. *International Journal of Biometeorology*, **57**, 749-758.
- 431 Di Bella C, Faivre R, Ruget F *et al.* (2004) Remote sensing capabilities to estimate pasture production in France.  
432 *International Journal of Remote Sensing*, **25**, 5359-5372.
- 433 Editorial Board of Vegetation Map of China Cas (2001) 1:1000,000 Vegetation Atlas of China. (ed Hou XY) pp  
434 Page, Beijing, China, Science Press.

- 435 Fu Y, Piao S, Op De Beeck M, Cong N, Menzel A, Janssens IA (2014a) Recent spring phenology shifts in Central  
436 Europe based on multi-scale observations. *Global Ecology and Biogeography*, **In Press**, DOI:  
437 10.1111/geb.12210.
- 438 Fu YH, Piao S, Zhao H *et al.* (2014b) Unexpected role of winter precipitation in determining heat requirement for  
439 spring vegetation green-up at northern-middle and high latitudes. *Global Change Biology*, **In Press**, doi:  
440 10.1111/gcb.12610.
- 441 Ganguly S, Friedl MA, Tan B, Zhang XY, Verma M (2010) Land surface phenology from MODIS: Characterization  
442 of the Collection 5 global land cover dynamics product. *Remote Sensing Of Environment*, **114**,  
443 1805-1816.
- 444 Gao YC, Liu MF (2013) Evaluation of high-resolution satellite precipitation products using rain gauge  
445 observations over the Tibetan Plateau. *Hydrology and Earth System Sciences*, **17**, 837-849.
- 446 Garonna I, De Jong R, De Wit AJW, Múcher CA, Schmid B, Schaepman M (2014) Strong contribution of autumn  
447 phenology to changes in satellite-derived growing season length estimates across Europe (1982–2011).  
448 *Global Change Biology*, **In Press**, doi: 10.1111/gcb.12625.
- 449 Hanninen H, Kramer K (2007) A framework for modelling the annual cycle of trees in boreal and temperate  
450 regions. *Silva Fennica*, **41**, 167-205.
- 451 He J (2010) Development of surface meteorological dataset of China with high temporal and spatial resolution.  
452 Unpublished M. S. Chin. Acad. of Sci., Beijing, China.
- 453 Huete A, Didan K, Miura T, Rodriguez EP, Gao X, Ferreira LG (2002) Overview of the radiometric and biophysical  
454 performance of the MODIS vegetation indices. *Remote Sensing Of Environment*, **83**, 195-213.
- 455 Huffman GJ, Adler RF, Bolvin DT *et al.* (2007) The TRMM multisatellite precipitation analysis (TMPA):  
456 Quasi-global, multiyear, combined-sensor precipitation estimates at fine scales. *Journal of*

- 457 *Hydrometeorology*, **8**, 38-55.
- 458 Hwang T, Band LE, Miniati CF, Song C, Bolstad PV, Vose JM, Love JP (2014) Divergent phenological response to  
459 hydroclimate variability in forested mountain watersheds. *Global Change Biology*, **20**, 2580-2595.
- 460 IPCC (2007) *Climate Change 2007: The physical science basis*, New York, Cambridge University Press.
- 461 Jeong S-J, Ho C-H, Gim H-J, Brown ME (2011) Phenology shifts at start vs. end of growing season in temperate  
462 vegetation over the Northern Hemisphere for the period 1982-2008. *Global Change Biology*, **17**,  
463 2385-2399.
- 464 Jeong SJ, Medvigy D, Shevliakova E, Malyshev S (2012) Uncertainties in terrestrial carbon budgets related to  
465 spring phenology. *Journal of Geophysical Research-Biogeosciences*, **117**, doi: 10.1029/2011jg001868.
- 466 Kato T, Tang YH, Gu S, Hirota M, Du MY, Li YN, Zhao XQ (2006) Temperature and biomass influences on  
467 interannual changes in CO<sub>2</sub> exchange in an alpine meadow on the Qinghai-Tibetan Plateau. *Global  
468 Change Biology*, **12**, 1285-1298.
- 469 Klein JA, Hopping KA, Yeh ET, Nyima Y, Boone RB, Galvin KA (2014) Unexpected climate impacts on the Tibetan  
470 Plateau: Local and scientific knowledge in findings of delayed summer. *Global Environmental Change*,  
471 **28**, 141-152.
- 472 Liu H, Tian F, Hu HC, Hu HP, Sivapalan M (2013) Soil moisture controls on patterns of grass green-up in Inner  
473 Mongolia: an index based approach. *Hydrology and Earth System Sciences*, **17**, 805-815.
- 474 Maisongrande P, Duchemin B, Dedieu G (2004) VEGETATION/SPOT: an operational mission for the Earth  
475 monitoring; presentation of new standard products. *International Journal of Remote Sensing*, **25**, 9-14.
- 476 Menzel A, Sparks TH, Estrella N *et al.* (2006) European phenological response to climate change matches the  
477 warming pattern. *Global Change Biology*, **12**, 1969-1976.
- 478 Mod13a1-Quality (2011) MOD13A1 VI Quality. pp Page,

- 479 [https://lpdaac.usgs.gov/products/modis\\_products\\_table/mod13a1](https://lpdaac.usgs.gov/products/modis_products_table/mod13a1).
- 480 Murray M, Cannell M, Smith R (1989) Date of budburst of fifteen tree species in Britain following climatic  
481 warming. *Journal of Applied Ecology*, **26**, 693-700.
- 482 Myneni RB, Keeling CD, Tucker CJ, Asrar G, Nemani RR (1997) Increased plant growth in the northern high  
483 latitudes from 1981 to 1991. *Nature*, **386**, 698-702.
- 484 Obrist D, Verburg PSJ, Young MH, Coleman JS, Schorran DE, Arnone JA (2003) Quantifying the effects of  
485 phenology on ecosystem evapotranspiration in planted grassland mesocosms using EcoCELL  
486 technology. *Agricultural and Forest Meteorology*, **118**, 173-183.
- 487 Peng S, Piao S, Ciais P *et al.* (2013) Asymmetric effects of daytime and night-time warming on Northern  
488 Hemisphere vegetation. *Nature*, **501**, 88-92.
- 489 Penuelas J, Filella I, Zhang XY *et al.* (2004) Complex spatiotemporal phenological shifts as a response to rainfall  
490 changes. *New Phytologist*, **161**, 837-846.
- 491 Piao S, Cui M, Chen A, Wang X, Ciais P, Liu J, Tang Y (2011) Altitude and temperature dependence of change in  
492 the spring vegetation green-up date from 1982 to 2006 in the Qinghai-Xizang Plateau. *Agricultural and  
493 Forest Meteorology*, **151**, 1599-1608.
- 494 Piao S, Fang JY, Zhou LM, Ciais P, Zhu B (2006) Variations in satellite-derived phenology in China's temperate  
495 vegetation. *Global Change Biology*, **12**, 672-685.
- 496 Piao S, Tan K, Nan H *et al.* (2012) Impacts of climate and CO<sub>2</sub> changes on the vegetation growth and carbon  
497 balance of Qinghai-Tibetan grasslands over the past five decades. *Global and Planetary Change*,  
498 **98-99**, 73-80.
- 499 Piao SL, Friedlingstein P, Ciais P, Viovy N, Demarty J (2007) Growing season extension and its impact on  
500 terrestrial carbon cycle in the Northern Hemisphere over the past 2 decades. *Global Biogeochemical*



- 501           *Cycles*, **21**, GB3018, doi:3010.1029/2006GB002888.
- 502 Rahman H, Dedieu G (1994) SMAC - a simplified method for the atmospheric correction of satellite  
503           measurements in the solar spectrum. *International Journal of Remote Sensing*, **15**, 123-143.
- 504 Reynolds JF, Smith DM, Lambin EF *et al.* (2007) Global desertification: building a science for dryland  
505           development. *Science*, **316**, 847-851.
- 506 Richardson AD, Anderson RS, Arain MA *et al.* (2012) Terrestrial biosphere models need better representation of  
507           vegetation phenology: results from the North American Carbon Program Site Synthesis. *Global Change*  
508           *Biology*, **18**, 566-584.
- 509 Richardson AD, Black AT, Ciais P *et al.* (2010) Influence of spring and autumn phenological transitions on forest  
510           ecosystem productivity. *Philosophical Transactions of the Royal Society B: Biological Sciences*, **365**,  
511           3227-3246.
- 512 Richardson AD, Keenan TF, Migliavacca M, Ryu Y, Sonnentag O, Toomey M (2013) Climate change, phenology,  
513           and phenological control of vegetation feedbacks to the climate system. *Agricultural and Forest*  
514           *Meteorology*, **169**, 156-173.
- 515 Sheffield J, Goteti G, Wood EF (2006) Development of a 50-year high-resolution global dataset of meteorological  
516           forcings for land surface modeling. *Journal of Climate*, **19**, 3088-3111.
- 517 Shen M, Tang Y, Chen J, Yang W (2012) Specification of thermal growing season in temperate China from 1960  
518           to 2009. *Climatic Change*, **114**, 793-798.
- 519 Shen M, Tang Y, Chen J *et al.* (2014a) Earlier-Season Vegetation Has Greater Temperature Sensitivity of Spring  
520           Phenology in Northern Hemisphere. *PLoS ONE*, **9**, e88178.
- 521 Shen M, Tang Y, Chen J, Zhu X, Zheng Y (2011) Influences of temperature and precipitation before the growing  
522           season on spring phenology in grasslands of the central and eastern Qinghai-Tibetan Plateau.

- 523            *Agricultural and Forest Meteorology*, **151**, 1711-1722.
- 524    Shen M, Tang Y, Klein J, Zhang P, Gu S, Shimono A, Chen J (2008) Estimation of aboveground biomass using in  
525            situ hyperspectral measurements in five major grassland ecosystems on the Tibetan Plateau. *Journal of*  
526            *Plant Ecology*, **1**, 247-257.
- 527    Shen M, Zhang G, Cong N, Wang S, Kong W, Piao S (2014b) Increasing altitudinal gradient of spring vegetation  
528            phenology during the last decade on the Qinghai–Tibetan Plateau. *Agricultural and Forest*  
529            *Meteorology*, **189–190**, 71-80.
- 530    Shen MG, Chen J, Zhu XL, Tang YH, Chen XH (2010) Do flowers affect biomass estimate accuracy from NDVI and  
531            EVI? *International Journal of Remote Sensing*, **31**, 2139-2149.
- 532    Studer S, Stockli R, Appenzeller C, Vidale PL (2007) A comparative study of satellite and ground-based  
533            phenology. *International Journal of Biometeorology*, **51**, 405-414.
- 534    Tan K, Ciaia P, Piao S *et al.* (2010) Application of the ORCHIDEE global vegetation model to evaluate biomass and  
535            soil carbon stocks of Qinghai-Tibetan grasslands. *Global Biogeochem. Cycles*, **24**, GB1013.
- 536    Tucker CJ, Fung IY, Keeling CD, Gammon RH (1986) Relationship between Atmospheric CO<sub>2</sub> Variations and a  
537            Satellite-Derived Vegetation Index. *Nature*, **319**, 195-199.
- 538    Vgt-Faq (2012) FAQ About the VGT products.    pp Page, <http://www.vgt.vito.be/faqnew/>.
- 539    Wang S, Duan J, Xu G *et al.* (2012) Effects of warming and grazing on soil N availability, species composition, and  
540            ANPP in an alpine meadow. *Ecology*, **93**, 2365-2376.
- 541    Wylie BK, Meyer DJ, Tieszen LL, Mannel S (2002) Satellite mapping of surface biophysical parameters at the  
542            biome scale over the North American grasslands - A case study. *Remote Sensing Of Environment*, **79**,  
543            266-278.
- 544    Xu ZX, Gong TL, Li JY (2008) Decadal trend of climate in the Tibetan Plateau—regional temperature and

- 545 precipitation. *Hydrological Processes*, **22**, 3056-3065.
- 546 Yatagai A, Arakawa O, Kamiguchi K, Kawamoto H, Nodzu MI, Hamada A (2009) A 44-Year Daily Gridded  
547 Precipitation Dataset for Asia Based on a Dense Network of Rain Gauges. *Sola*, **5**, 137-140.
- 548 You QL, Fraedrich K, Ren GY, Pepin N, Kang SC (2013) Variability of temperature in the Tibetan Plateau based on  
549 homogenized surface stations and reanalysis data. *INTERNATIONAL JOURNAL OF CLIMATOLOGY*, **33**,  
550 1337-1347.
- 551 Yu FF, Price KP, Ellis J, Shi PJ (2003) Response of seasonal vegetation development to climatic variations in  
552 eastern central Asia. *Remote Sensing Of Environment*, **87**, 42-54.
- 553 Yu HY, Luedeling E, Xu JC (2010) Winter and spring warming result in delayed spring phenology on the Tibetan  
554 Plateau. *Proceedings of the National Academy of Sciences of the United States of America*, **107**,  
555 22151-22156.
- 556 Zhang G, Zhang Y, Dong J, Xiao X (2013) Green-up dates in the Tibetan Plateau have continuously advanced  
557 from 1982 to 2011. *Proceedings of the National Academy of Sciences of the United States of America*,  
558 **110**, 4309-4314.
- 559 Zhang X, Friedl MA, Schaaf CB *et al.* (2003) Monitoring vegetation phenology using MODIS. *Remote Sensing Of*  
560 *Environment*, **84**, 471-475.
- 561 Zhang XY, Friedl MA, Schaaf CB (2006) Global vegetation phenology from Moderate Resolution Imaging  
562 Spectroradiometer (MODIS): Evaluation of global patterns and comparison with in situ measurements.  
563 *Journal of Geophysical Research-Biogeosciences*, **111**, G04017, doi:04010.01029/02006JG000217.
- 564 Zhang XY, Friedl MA, Schaaf CB, Strahler AH (2004) Climate controls on vegetation phenological patterns in  
565 northern mid- and high latitudes inferred from MODIS data. *Global Change Biology*, **10**, 1133-1145.
- 566 Zhang XY, Friedl MA, Schaaf CB, Strahler AH, Liu Z (2005) Monitoring the response of vegetation phenology to

567 precipitation in Africa by coupling MODIS and TRMM instruments. *Journal of Geophysical*

568 *Research-Atmospheres*, **110**, D12103, 12110.11029/12004JD005263

569 Zhang XY, Tarpley D, Sullivan JT (2007) Diverse responses of vegetation phenology to a warming climate.

570 *Geophysical Research Letters*, **34**, L19405, doi:19410.11029/12007GL031447.

571

572

573

574 **Figure captions**

575

## 576 Fig. 1

577 Spatial distribution of sensitivity of SOS to preseason mean temperature (day °C<sup>-1</sup>). (a), the  
578 sensitivity was calculated for each pixel using satellite-derived SOS and temperature and  
579 precipitation developed by Data Assimilation and Modeling Center for Tibetan Multi-spheres,  
580 Institute of Tibetan Plateau Research, Chinese Academy of Sciences. Top inset shows the  
581 pixels with significantly ( $P < 0.05$ ) negative (green) and positive (red) sensitivities. The  
582 bottom right inset shows the frequency distributions of corresponding sensitivity. Grey  
583 indicates no SOS data. (b), similar to (a), but using temperature and precipitation observed at  
584 meteorological stations.

585

## 586 Fig. 2

587 Similar to Fig. 1, but for sensitivity of SOS to preseason precipitation (day mm<sup>-1</sup>).

588

## 589 Fig. 3

590 (a) Variations in sensitivity of SOS to preseason mean temperature along the spatial gradient  
591 of long-term average precipitation. The black thick curve shows the values averaged from all  
592 the pixels for each 10-mm bin of long-term average precipitation, and the gray thick curve  
593 shows the average of sensitivity significant at  $P < 0.05$  level. Error bar shows standard error  
594 of the mean (SEM). The partial correlation coefficient near the black thick curve was between  
595 the temperature sensitivity of SOS and long-term average precipitation while accounting for

596 CD and MAT. The right inset shows the frequency distributions of corresponding long-term  
597 average precipitation. The left inset shows the spatial partial correlation coefficient between  
598 temperature sensitivity of SOS and long-term average precipitation by setting MAT and CD at  
599 the controlling variables, using temperature and precipitation observed at meteorological  
600 stations. (b), similar to (a), but for the sensitivity of SOS to pre-season precipitation. \*\*\*  
601 indicates significance at  $P < 0.01$  level.

602

603 Fig. 4

604 (a) Spatial distribution of inter-annual partial correlation coefficient between GDD and  
605 pre-season precipitation with setting CD as the controlling variable. The inset shows the  
606 frequency distributions of corresponding correlation coefficient. Correlation coefficient values  
607 of  $\pm 0.5$ ,  $\pm 0.58$ ,  $\pm 0.71$  correspond to significance levels of  $P = 0.10$ ,  $0.05$ , and  $0.01$ ,  
608 respectively. (b) Similar to (a), but using temperature and precipitation observed at  
609 meteorological stations. (c) Variations in the inter-annual partial correlation coefficient along  
610 the spatial gradient of long-term average precipitation. The black thick curve shows the values  
611 averaged from all the pixels for each 10-mm bin of long-term average precipitation, and the  
612 gray thick curve shows the average of partial correlation coefficient significant at  $P < 0.05$   
613 level. The partial correlation coefficient near the black thick curve was between the  
614 inter-annual partial correlation coefficient between GDD and pre-season precipitation and  
615 long-term average precipitation while accounting for CD and MAT. Error bar shows SEM.  
616 The inset shows the spatial partial correlation coefficient between inter-annual partial  
617 correlation coefficient between GDD and precipitation and long-term average precipitation by

618 setting MAT and CD at the controlling variables, using temperature and precipitation  
619 observed at meteorological stations. \*\*\* and \*\* indicate significance at  $P < 0.01$  and  $P < 0.05$   
620 levels, respectively.

621

622 Fig. 5

623 (a) Spatial distribution of multi-yearly averaged GDD ( $^{\circ}\text{C day}$ ). The inset shows the  
624 frequency distributions of corresponding GDD. (b) The black thick curve shows variations in  
625 multi-yearly averaged GDD and the gray curve shows the MAT along the spatial gradient of  
626 long-term average precipitation. Error bar shows SEM. The partial correlation coefficient near  
627 the black thick curve was between GDD and long-term average precipitation while  
628 accounting for CD and MAT. The inset shows the spatial partial correlation between  
629 multi-yearly averaged GDD and long-term average precipitation by setting MAT and CD as  
630 the controlling variables, using temperature and precipitation observed at meteorological  
631 stations. \*\*\* indicates significance at  $P < 0.01$  level.

632

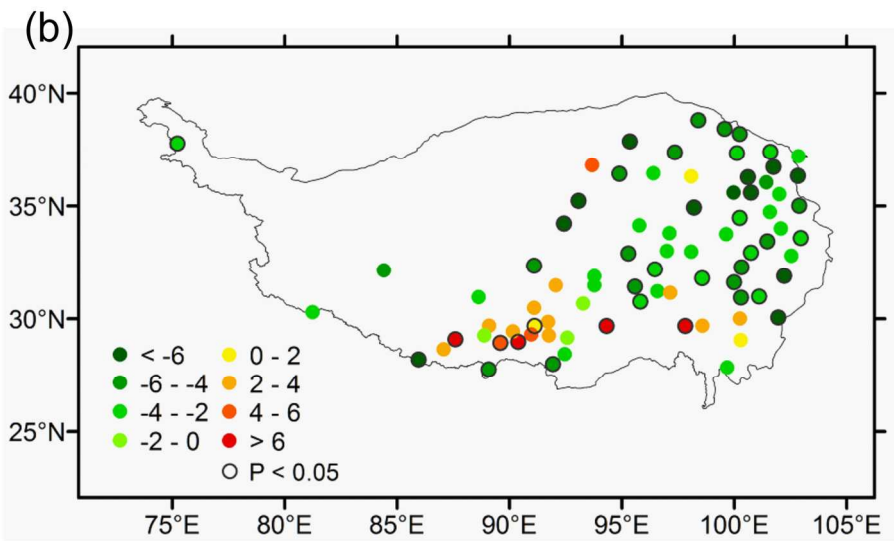
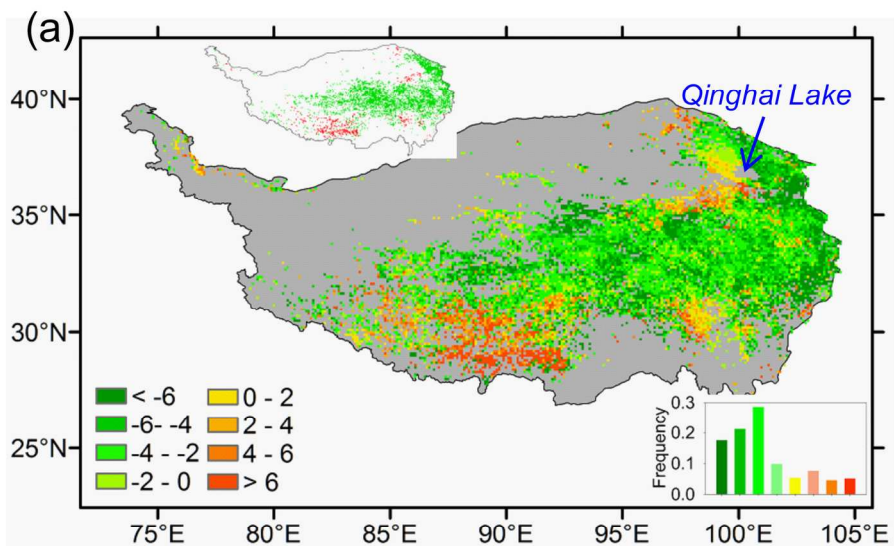
633 Fig. 6

634 Comparisons of averages of long-term average precipitation, sensitivities of SOS to pre-season  
635 mean temperature and precipitation, inter-annual partial correlation coefficient between GDD  
636 and precipitation, and multi-yearly averaged GDD, among the three major vegetation types of  
637 the Tibetan Plateau. The solid curves show the values averaged from all the pixels for each  
638 vegetation type, and the dashed curves show the average of significant ( $P < 0.05$ ) items listed  
639 in the right y-axis labels. Alpine veg includes alpine tundra, alpine cushion, and alpine sparse

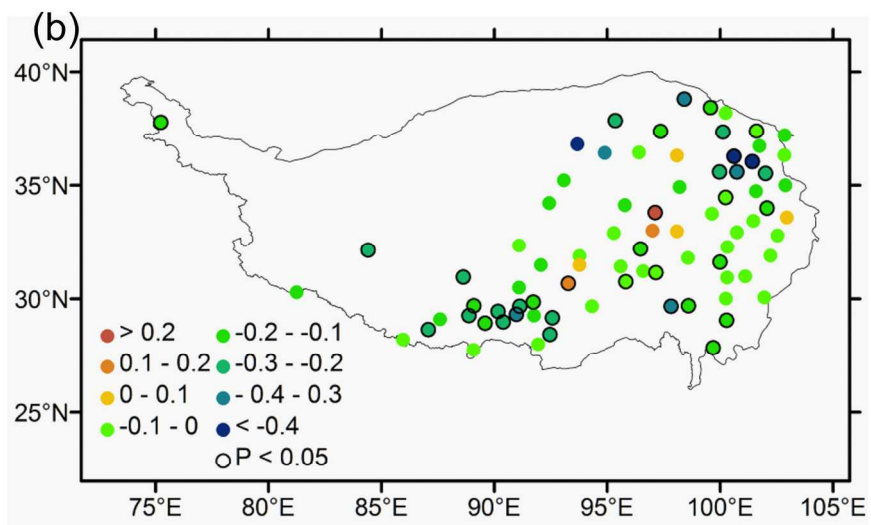
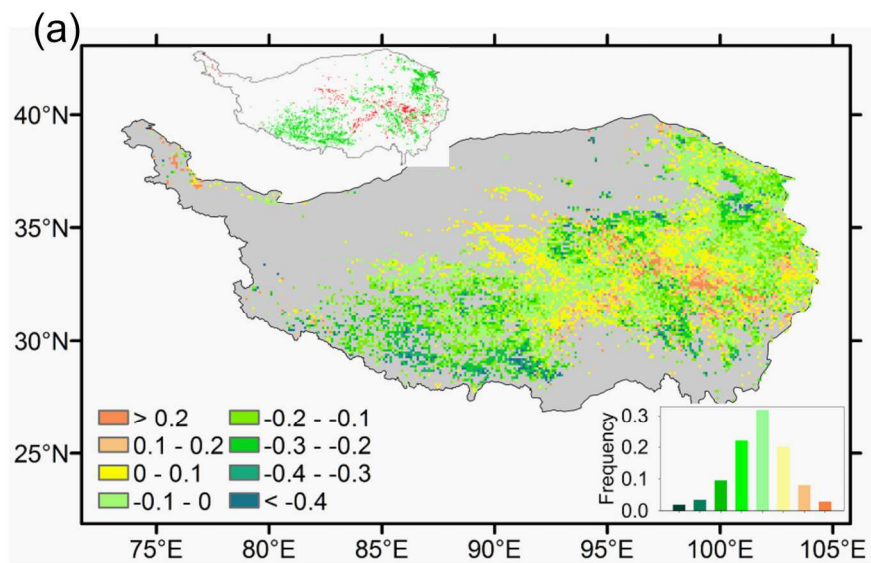
640 vegetation according to Editorial Board of Vegetation Map of China CAS (2001).

641

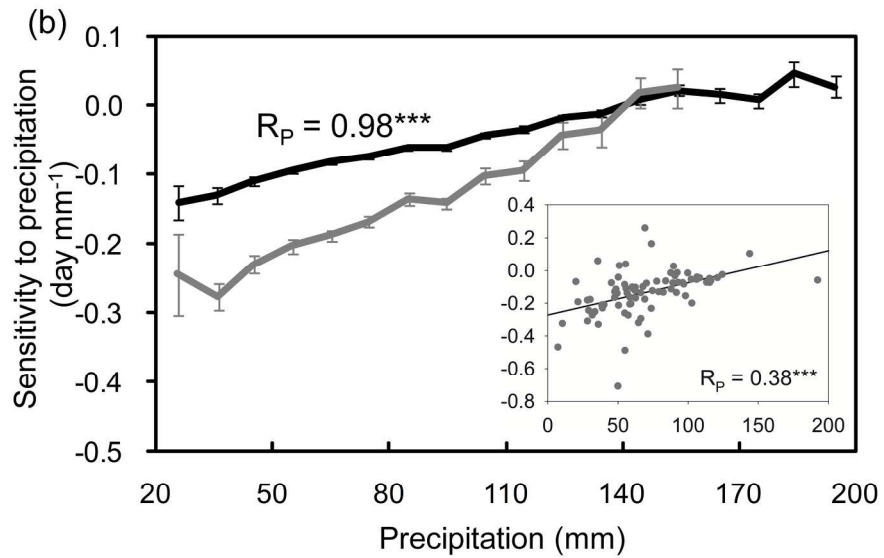
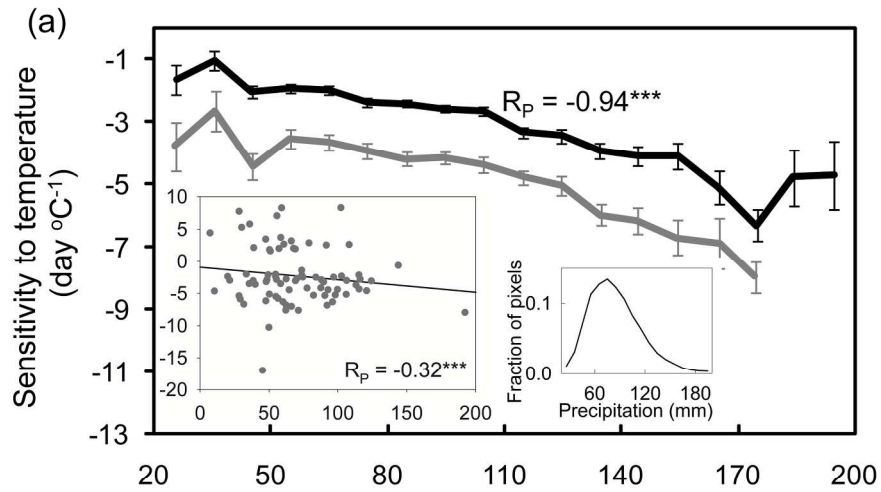




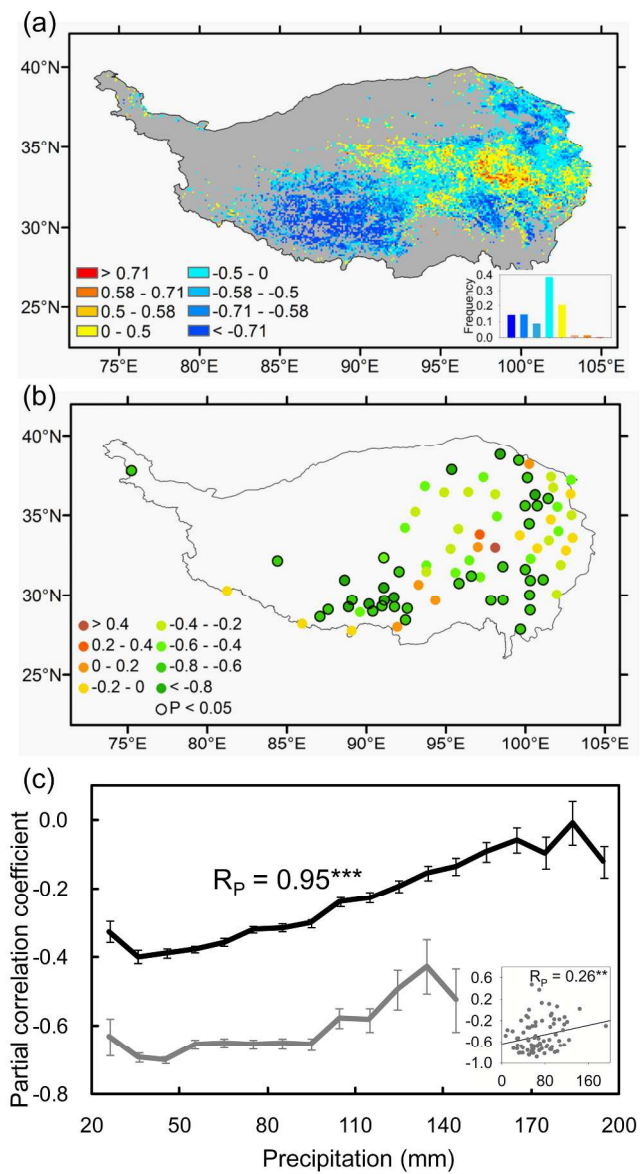
161x203mm (300 x 300 DPI)



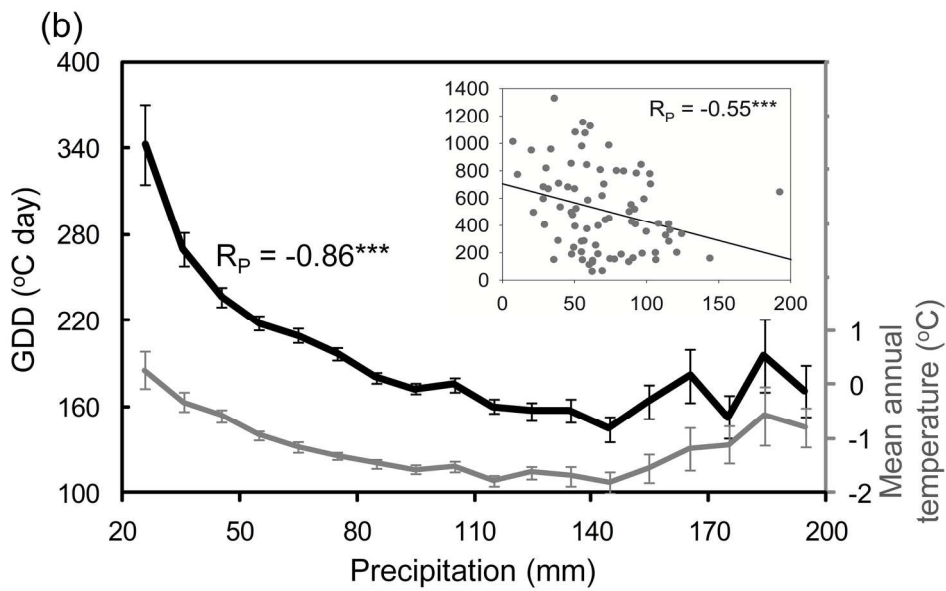
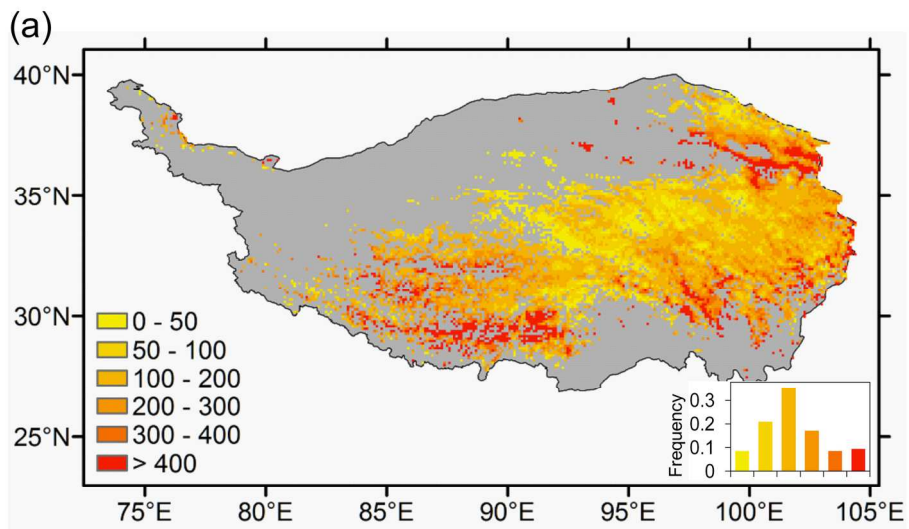
166x217mm (300 x 300 DPI)



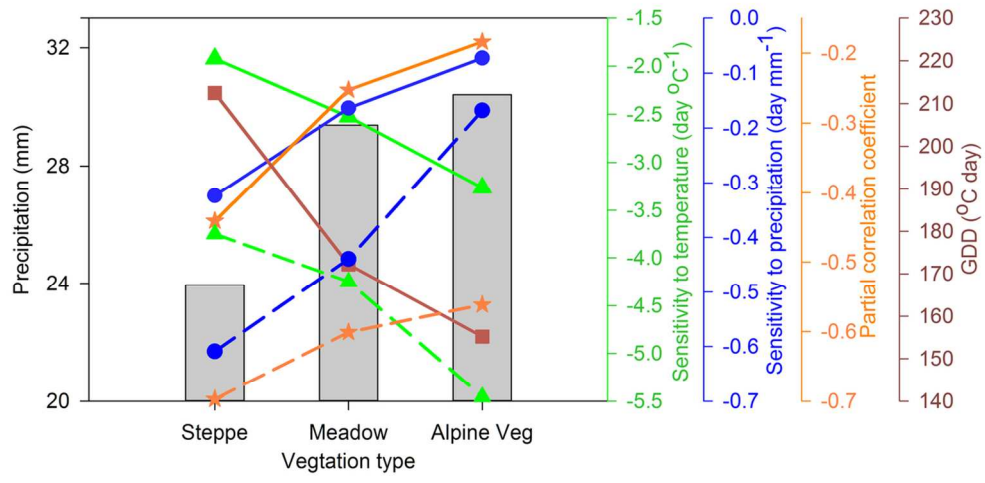
203x258mm (300 x 300 DPI)



238x423mm (300 x 300 DPI)



184x219mm (300 x 300 DPI)



114x55mm (300 x 300 DPI)